A Novel Sensing Scheme for the Displacement of Electrostatically Actuated Microcantilevers

Mariateresa Napoli   Craig Olroyd   Bassam Bamieh   Kimberly Turner

Abstract— We present the design and implementation of a novel sensing scheme to reconstruct the displacement of electrostatically actuated microcantilevers that are used in atomic force microscopy. Our approach proposes to *estimate* rather than *measure* directly the displacement, by means of an observer that uses the current through the capacitive cantilever as an input. In particular, we formulate the observer problem as an $\mathcal{H}_\infty$ optimal filtering problem for periodic systems. We show here our first experimental results regarding the implementation of this sensing scheme, which includes a custom made off-chip circuit to measure very small currents (few pA) at high frequencies (≈ 100kHz).

I. INTRODUCTION

The recent advances in the field of miniaturization and microfabrication have paved the way for a new range of applications, bringing along the promise of unprecedented levels of performance, attainable at a limited cost, thanks to the use of batch processing techniques.

In particular, scanning probe devices have proven to be extremely versatile instruments, with applications that range from surface imaging at the atomic scale, to ultra high density data storage and retrieval, to biosensors, and to nanolithography.

However, in order to achieve the anticipated results in terms of performance, an increase in throughput is required. In this respect, much of the research effort has been focused on the design of integrated detection schemes, which offer moreover the advantage of compactness.

The most common solutions make use of the piezoresistive [1], [2], piezoelectric [3], [4], [5], thermal expansion [6] or capacitive effects [7], [8], [9]. The device that we propose is an electrostatically actuated microcantilever. More precisely, in our design the microcantilever constitutes the movable plate of a variable capacitor. Its displacement is controlled by the voltage applied across the plates and current is measured directly by a transimpedance amplifier.

A major advantage of capacitive detection, is the fact that it offers both electrostatic actuation as well as integrated detection, without the need for an additional position sensing device. The common scheme used in capacitive detection is to apply a second AC voltage at a frequency much higher than the mechanical bandwidth of the cantilever. The current output at that frequency is then used to estimate the capacitance, and consequently the cantilever position.

All the authors are with the Department of Mechanical Engineering, University of California, Santa Barbara CA 93106, U.S.A., {napoli,craig,turner,bamieh}@engr.ucsb.edu

This sensing scheme is the simplest position detection scheme available, however, it is widely believed to be less accurate than optical levers or piezoresistive sensing. We propose a novel scheme that avoids the use of a high frequency probing signal by the use of a dynamical state observer whose input is the current through the capacitive cantilever. This approach that we call "indirect" sensing, has the advantage of allowing for compact devices, by removing the usually cumbersome apparatus used in optical sensing techniques [10], [11], [12], [13]. By using an optimal observer, or by tuning the observers gains, it is conceivable that a high fidelity position measurement can be obtained, thus improving resolution in atomic force microscopy applications.
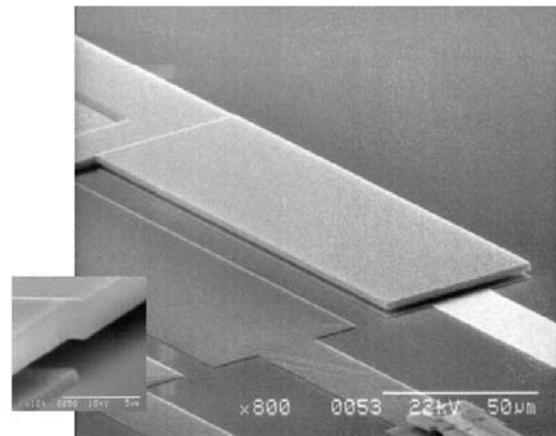
Fig. 1. SEM micrograph of one of our electrostatically actuated microcantilevers, with inset showing details of the mechanical connection to the base.

In this paper, we present a model for an electrostatically actuated microcantilever. Using simple parallel plate theory and for the common case of sinusoidal excitation, it turns out that its dynamics are governed by a second order linear periodic differential equation. We formulate the observer problem as an $\mathcal{H}_\infty$ optimal filtering problem for periodic systems. We show our first experimental results regarding the implementation of this sensing scheme, which includes a custom made off-chip circuit to measure very small currents (few pA) at high frequencies (≈ 100kHz). These results

show the potential of the methodology proposed: by reducing measurement noise (with an on-chip implementation of the circuit or better shielding) it is conceivable that we will be able to achieve very high accuracy. The extension of these results to array configurations is also the subject of our current research.

II. MICROCANTILEVER MODEL

The device that we have considered is shown in Fig.1. It consists of two adjacent electrically conductive beams forming the two plates of a capacitor. One of the beams is rigid, while the other (top cantilever, visible in the picture) is fairly soft and represents the movable part of the structure. In particular, the device shown in Fig.1 was fabricated using the MUMPS/CRONOS process. The plates are $200\mu m \times 50\mu m \times 2\mu m$ highly doped polysilicon and the gap between them is of about $2\mu m$.

When the length of the cantilever is much bigger than its distance from the bottom plate, the capacitance can be approximated as

$$C(z) = \frac{\epsilon_o A}{d - z},$$

where $\epsilon_o = 8.85 \ 10^{-12} As/Vm$ is the permittivity in vacuum, A is the area of the plates, d is the gap between them and z is the vertical displacement of the cantilever from its rest position.

The electrostatic attractive force, F_{elec}, between the capacitor plates generated by applying a voltage $V(t) = V_o \cos \omega_o t$, is given by

$$F_{elec} = \frac{1}{2}\frac{\epsilon_o A}{d^2}\frac{V^2(t)}{(1-\frac{z}{d})^2} \approx \frac{1}{2}\frac{\epsilon_o A}{d^2}(1+2\frac{z}{d})V^2(t),$$

where the approximation holds for $\frac{z}{d} << 1$.

Hence, it follows that the linearized dynamics of an electrostatically actuated cantilever are described by the following system of periodic differential equations

$$\dot{x} = \begin{bmatrix} 0 & 1 \\ -a + 2q\cos 2\omega_o t & -c \end{bmatrix} x + \begin{bmatrix} 0 \\ b_1 \end{bmatrix} u^2$$
$$= A(t)x + Bu^2, \quad (1)$$

where $x = [z \ \ \dot{z}]^T$ is the vector of vertical position and velocity of the cantilever. The constants in (1) are $a = \frac{k}{m\omega_o^2} - \frac{1}{2}\frac{\epsilon_o A V_o^2}{md^3\omega_o^2}$, with k and m respectively spring constant and mass of the cantilever; $q = \frac{\epsilon_o A V_o^2}{4md^3\omega_o^2}$; $c = \frac{2\xi}{\omega_o}\sqrt{\frac{k}{m}}$ with ξ damping coefficient; and $b_1 = q \ d$. The model has been experimentally validated and the value of all the parameters experimentally identified [14], [15]. In particular, the resonant frequency of these cantilevers is between $50 - -53$ kHz and their quality factor in vacuum is $Q \approx 2000$.

We consider the current through the capacitor plates as the output $y = \frac{d}{dt}[C(z)V(t)]$ of the system. For a sinusoidal input $V(t) = V_o \cos \omega_o t$, the first order approximation of y is given by

$$y = [c_1 \sin(\omega_o t) \ \ c_2\cos(\omega_o t)] x + c_o \sin(\omega_o t),$$
$$= C(t)x + v(t). \quad (2)$$

Here $c_o = \frac{\epsilon_o A V_o w_o}{d}$, $c_1 = -\frac{\epsilon_o A V_o w_o}{d^2}$ and $c_2 = \frac{\epsilon_o A V_o}{d^2}$.

Note from (2) that the current has two components : one that depends only on the input

$$i_{inp} = v(t),$$

and one carrying the information about the cantilever dynamics

$$i_{mot} = c_1 \sin(\omega_o t)x + c_2\cos(\omega_o t)\dot{x}. \quad (3)$$

This latter is the "useful" component that the observer uses to reconstruct the cantilever displacement.

III. OPTIMAL OBSERVER DESIGN

In this section we present the design of the observer, which is at the core of our sensing scheme. The observer is a dynamical system that provides an estimate $\hat{x}$ of the cantilever displacement based on the measurement of the current generated. This approach to sensing is particularly advantageous from the point of view of implementation, as it requires a simpler circuitry. As a matter of fact, the extraction of the desired information is left to a software elaboration of the measurements.

The observer problem in the Linear Fractional Transformation (LFT) framework can be formulated as an $\mathcal{H}_\infty$ filtering problem, by defining the variable $z := x - \hat{x}$ (estimation error), and considering the generalized plant shown in Fig.2 and described by

$$G_{gen} := \left[\begin{array}{c|cc} A(t) & B_1 & 0 \\ \hline C_1 & 0 & D_{12} \\ C_2(t) & D_{21} & 0 \end{array}\right] = \left[\begin{array}{c|cc} A(t) & [M \ 0] & 0 \\ \hline I & 0 & -I \\ C(t) & [0 \ N] & 0 \end{array}\right],$$
$$(4)$$

where the exogenous input $w = [d \ n]^T$ represents process and measurement noise, the matrices M and N are respectively the process and measurement noise weight, the matrices $A(t), C(t)$ are as in (1) and (2) and the input $u = \hat{x}$ is the output of the observer system [15]. Notice that we do not need to account for the signal v in (2): since it is a known function of the input, its presence does not affect the observer design.

In this framework, the optimal observer problem amounts to finding a dynamical system G_{obs} such that the $\mathcal{H}_\infty$ norm of the transfer function T_{zw} from w to z is minimized. If the system is time-invariant, and has the structure of (4), where $D_{21}'B_1 = 0$, than the optimal filter is an observer, whose gain L comes from the solution of an appropriate algebraic Riccati equation [16]. It turns out that a similar result holds in the time-varying case as well. The details have been presented in [15]. When the system is periodic, the algebraic Riccati equation is replaced by a periodic differential Riccati equation. If the periodic non-negative
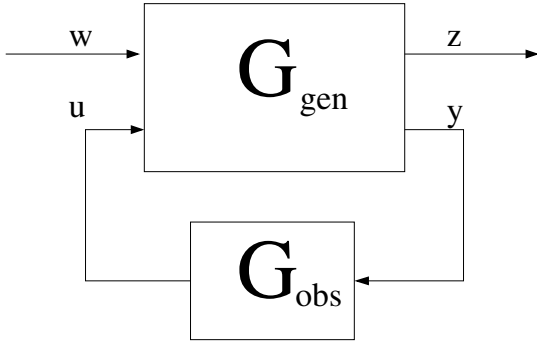
Fig. 2. A block diagram of the observer problem.

definite solution of this equation $P(t)$ is stabilizing, the optimal filter is given by

$$\dot{\hat{x}} = A(t)\hat{x} + \mathbf{P(t)C(t)}'[y(t) - C(t)\hat{x}].$$ (5)

IV. EXPERIMENTAL RESULTS

The implementation of the observer requires imprimis the measurement of the current through the cantilever and in particular of its motional component. In the normal mode of operation the cantilever will be driven close to its resonant frequency (about 50 kHz). From (1) and (2) note that when the input is a sinusoidal signal at ω_o, so are x and $\dot{x}$. Hence, the current y has two frequency components: i_{inp} at ω_o and i_{mot} at $2\omega_o$. In particular, in the linear regime of operation, the amplitude of i_{mot} is in the order of few picoamperes, and about two to three orders of magnitude smaller than the amplitude of i_{inp}.

It turned out that there are no off-the-shelf instruments able to perform the measurement of such a small current at such a high frequency. The next section describes the circuit we have designed to perform the measurement.

A. Circuit Design
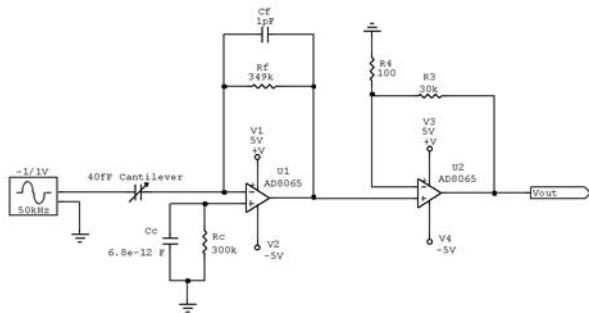
Fig. 3. Schematic diagram of the circuit to measure the current.

Figure 3 shows the schematic of the amplifier circuit used to measure the current. The design employs two amplification stages that achieve a current-to-voltage gain of 10^8 with a bandwidth of 300kHz. The first stage is a transimpedence amplifier that uses an AD8065 wideband opamp. The non-inverting input is balanced by R_c and C_c to minimize the offset produced by the amplifiers input bias current. The net transimpedence for the circuit is $R_t = R_f(1 + R3/R4)$ and the current-to-voltage response is

$$V_{out} = R_t I_{in}.$$

A two stage amplifier was chosen due to the bandwidth limitations of high gain transimpedence amplifiers. In fact, by adding a second stage voltage amplifier, the feedback resistor R_f can be reduced to improve bandwidth, while still maintaining a high transimpedence value R_t. In particular, the value of R_f can be optimized as a function of bandwidth and overall gain [17]. Even though the second stage causes amplification of noise, the improvement in bandwidth outpaces the degradation of noise, up to the optimal bandwidth limit [17].

Fig. 4. Picture showing the PCB and the cantilever die during testing.

The primary limitations to implementing off-chip capacitive detection are the presence of parasitic capacitances and leakage currents. These are present both in the amplifier circuitry and printed circuit board (PCB). Minimizing the effect of parasitic capacitances is first achieved by use of a transimpedence amplifier for the first stage. This configuration holds the cantilevers output voltage to zero by the virtual ground of the opamp, which minimizes the excitation of stray capacitances at the amplifier input. Equally important is the physical layout of the first stage components. Figure 4 shows the 1cm device die mounted onto the PCB, both within one of our 24 pin IC carriers. As part of the design, we have located the device die as close as possible to the first stage input. By wirebonding the output of the cantilever directly to the first stage opamp input we minimize parasitic impedances.

PCB layout, insulating board materials and contaminants can all generate leakage currents equal to or larger than the currents we are trying to measure. Therefore we have isolated the first stage opamp input with a driven guard ring.

In the next section we present the experimental results obtained by the use of this circuit.

TABLE I

COMPARISON BETWEEN THE CANTILEVERS CHARACTERISTIC
PARAMETERS OBTAINED BY FITTING THE CURVES IN FIG.5.

	ω_r	ξ
Circuit	52983	$2.3942e^{-5}$
Vibrom.	52981	$2.4272e^{-5}$

whose existence in MEMS devices was first demonstrated in [21]. The interest from an engineering point of view for this phenomenon comes from the fact that it can greatly enhance the sensitivity of microdevices, which as their size reduces, find themselves operating closer to noise level [22].

B. Experimental Data Analysis
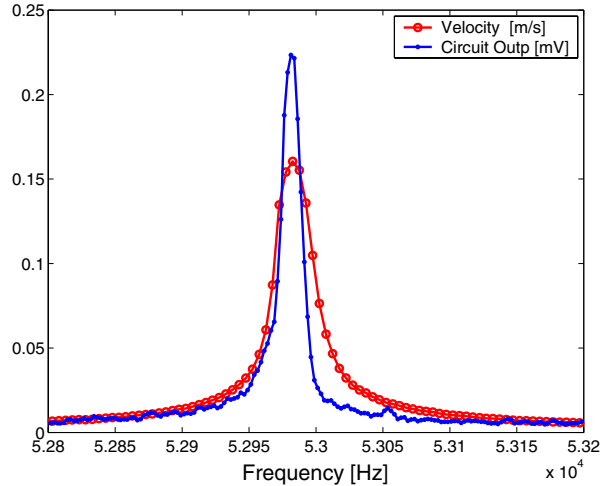
Fig. 5. Frequency response of the cantilever in terms of circuit output ('.' data), and vibrometer output ('o' data). The curves have been shifted horizontally to allow a comparison.

The experiments were conducted in vacuum ($p = 7\mathrm{mTorr}$) and the displacement of the cantilever was monitored using both the circuit described in the previous section and a laser vibrometer [13]. In particular, we have used the vibrometer to measure the out-of-plane velocity of the cantilever. Figure 5 shows the frequency response of the cantilever as measured by the circuit ('.') and the vibrometer ('o'). In these experiments the amplitude of the input voltage was small enough to allow a time-invariant approximation of equation (1). Note, in particular, that the output of the circuit in reality is at 2ω: the horizontal frequency axis has been shifted to allow a comparison with the vibrometer data. As can be seen, the two curves compare very well and by fitting them we have obtained a set of parameters in very good agreement, as shown in Table I.

The full periodic equation (1) that describes the cantilever is an instance of the famous Mathieu equation, whose stability properties have been extensively studied in the literature [18], [19], [20]. Its characteristic is that, in the absence of damping, particular combinations of the parameters a and q give rise to an unstable behavior. The presence of damping does not modify this behavior, but creates a threshold voltage, above which this parametric amplification can be induced. In [15] we showed that a single electrostatically actuated microcantilever can exhibit parametric resonance,
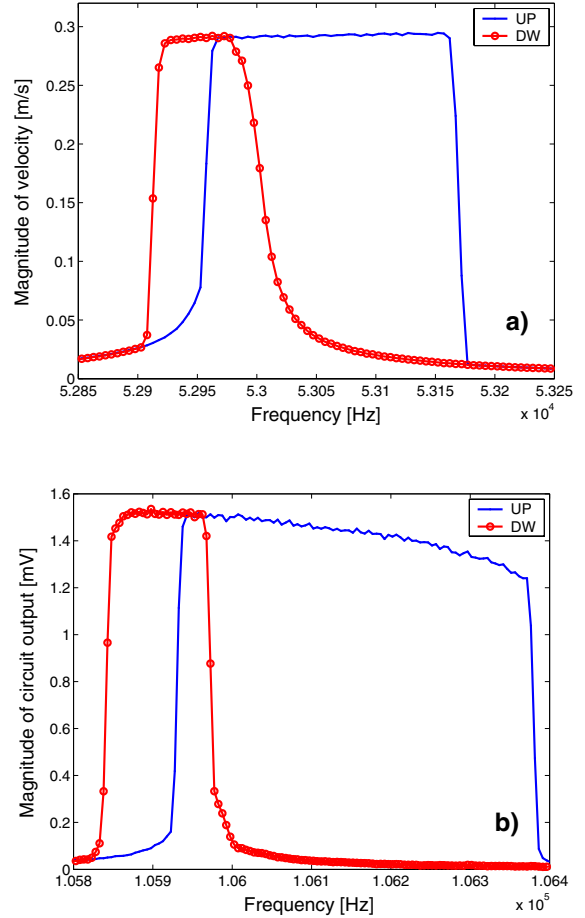
Fig. 6. Frequency response in parametric resonance: a) Vibrometer output, b) Circuit output due to i_{mot}.

Figure 6 reproduces the data of an experiment where the cantilever is excited in parametric resonance. The two curves reproduced in Fig.6 $a)$, $b)$ represent the data collected by sweeping the frequency from low to high (blue '.' points) and from high to low (red 'o' points). Each point in the plots represents the amplitude of the oscillation at that particular frequency: part $a)$ represents the vibrometer output, part $b)$ the circuit output. Notice the sharp transition of the amplitude both in $a)$ and $b)$ (vertical segment of '.' data) that marks the entrance into the parametric region. Since this transition always occurs for the same value of ω, related to the resonant frequency of the beam, the phenomenon has potentially many applications, from the realization of mechanical filters to extremely sensitive mass sensors. In particular, for the output of the circuit this jump occurs at exactly double the frequency of the jump

in velocity, as expected. Note also that the amplitude of the oscillation remains bounded. This is due to a nonlinear cubic term, of both mechanical and electrostatic origin [23], [24], [15].

The interested reader can find more details on this interesting phenomenon in microcantilevers in [14], [15]. Here we present this result to demonstrate the ability of the circuit to correctly reproduce the behavior of the cantilever.

C. Offline Implementation of the Observer
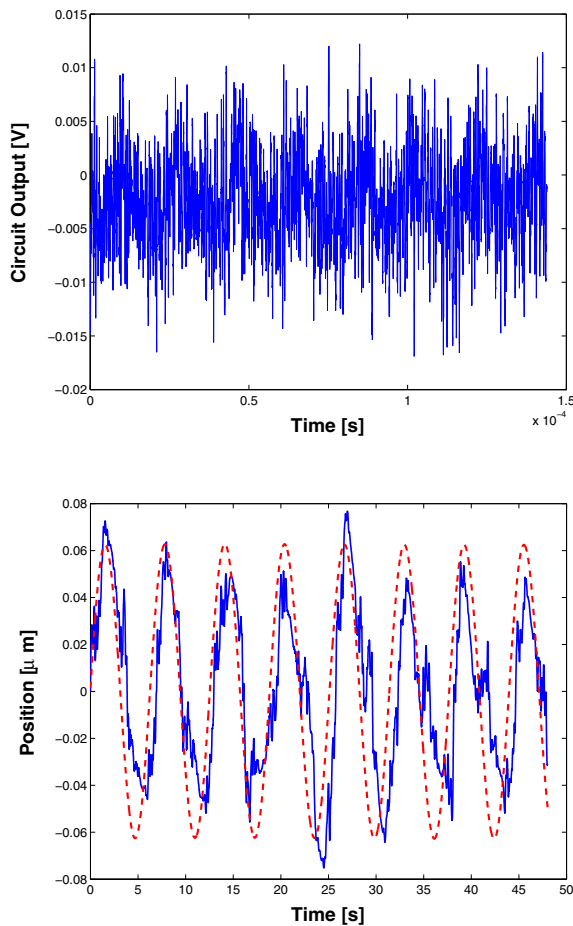
Fig. 7. a) Circuit output due to i_{mot}, b) Comparaison between estimated (solid line) and measured (dashed line) cantilever displacement.

Figure 7 shows the result of a first set of experiments regarding the offline implementation of the optimal observer, using the circuit described above for the measurement of the current. The input applied during this experiment was a sinusoidal function with amplitude $V_o = 300$ mV and frequency $f = 53100$ Hz.

In a previous section we noticed that i_{inp} and i_{mot} are respectively at ω_o and $2\omega_o$ and that i_{inp} is the useful component, carrying the information about the cantilever displacement. The small separation in frequency makes the

extraction of i_{mot} from the measurement of i difficult, since i_{inp} can be hardly filtered out of i.

Figure 7 a) represents the output of the circuit, once deprived of the component relative to i_{inp}. In this case, i_{inp} has been subtracted out of i, based on the model of the circuit and the identified parameters of the cantilever. Figure 7 b) compares the estimate of the cantilever displacement (solid line) obtained with an optimal observer, to measured data (dashed line). Notice how, in spite of the large amount of noise, the optimal observer is able to provide an estimate of the cantilever displacement, not too far off from its actual value. Even though the performance is not satisfactory yet, this result shows that indeed the sensing scheme proposed might be a viable alternative to existing devices. In particular we expect that, once we succeed in reducing the level of noise in the current measurement, this scheme will be able to offer comparable or better accuracy in the reconstruction of the cantilever displacement than the other available sensing schemes.

V. CONCLUSIONS

We have introduced the model of an electrostatically actuated cantilever, where we consider the current as the output signal. Based on this model we have designed an optimal observer, which we propose as the core of a new sensing scheme to reconstruct the displacement of the cantilever. Our approach, based on the idea of "indirect" sensing, has the potential of minimizing cost and size, by removing the usually cumbersome apparatus used in optical sensing techniques. We have offered the first results on the implementation of this sensing scheme. Although the estimate is still heavily affected by noise, the results presented give hope that the scheme proposed when slightly improved might be an interesting alternative to existing sensing schemes.

REFERENCES

[1] B. Chui et al., "Independent detection of vertical and lateral forces with a sidewall-implanted dual-axis piezoresistive cantilever," *Appl. Phys. Lett.*, vol. 72, no. 11, pp. 1388–1390, March 1998.
[2] M. Tortonese, R. Barrett, and C. Quate, "Atomic resolution with an atomic force microscope using piezoresistive detection," *Appl. Phys. Lett.*, vol. 62, no. 8, pp. 834–836, Feb. 1993.
[3] P. Gaucher et al., "Piezoelectric bimorph cantilever for actuation and sensing applications," *J. Phys. IV France*, vol. 8, pp. 235–238, 1998.
[4] T. Itoh, T. Ohashi, and T. Suga, "Piezoelectric cantilever array for multiprobe scanning force microscopy," in *Proc. of the IX Int. Workshop on MEMS, San Diego, CA*, pp. 451–455, 1996.
[5] S. Minne, S. Manalis, and C. Quate, "Parallel atomic force microscopy using cantilevers with integrated piezoresistive sensors and integrated piezoelectric actuators," *Appl. Phys. Lett.*, vol. 67, no. 26, pp. 3918–3920, 1995.
[6] Q. Huang and N. Lee, "A simple approach to characterizing the driving force of polysilicon laterally driven thermal microactuators," *Sensors & Actuators A-Physical*, vol. A80, no. 3, pp. 267–272, 15 March 2000.

[7] P. Attia et al., "Fabrication and characterization of electrostatically driven silicon microbeams," *Microelectronics J.*, vol. 29, pp. 641–44, 1998.

[8] N. Blanc et al., "Scanning force microscopy in the dynamic mode using microfabricated capacitive sensors," *J. Vac. Sci. Technol. B*, vol. 14, no. 2, pp. 901–905, Mar/Apr 1996.

[9] Y. Shiba et al., "Capacitive AFM probe for high speed imaging," *Trans. of the IEE of Japan*, vol. 118E, no. 12, pp. 647–50, 1998.

[10] S. Alexander et al., "An atomic-resolution atomic-force microscope implemented using an optical lever," *J. of Appl. Phys.*, vol. 65, pp. 164–67, 1989.

[11] G.Meyer and N.M.Amer, "Novel optical approach to atomic force microscopy," *Appl. Phys. Lett.*, vol. 53, pp. 1045–47, 1988.

[12] C.Schonenberg and S.F.Alvarado, "A differential interferometer for force microscopy," *Review of Scientific Instruments*, vol. 60, pp. 3131–34, 1989.

[13] K. Turner, P. Hartwell, and N. Macdonald, "Multi-dimensional MEMS motion characterization using laser vibrometry," in *Digest of Technical Papers Transducers'99, Sendai, Japan*, 1999.

[14] M. Napoli, R. Baskaran, K. Turner, and B.Bamieh, "Understanding mechanical domain parametric resonance in microcantilevers," in *Proc. of the IEEE 16th Annual Int. Conf. on MEMS, Kyoto JP*, pp. 169–172, 2003.

[15] M. Napoli, B. Bamieh, and K. Turner, "A capacitive microcantilever : Modelling, validation and estimation using current measurements," *J. of Dyn. Sys. Meas. and Control*, vol. 126, no. 2, pp. 319–26, June 2004.

[16] M.Green and D. Limebeer, *Linear Robust Control*. Prentice Hall, 1995.

[17] J. Graeme, *Photodiode amplifiers: Op Amp Solutions*. McGraw-Hill, New York, 1996.

[18] A. D.T.Mook, *Nonlinear Oscillations*. John Wiley & sons, New York, 1979.

[19] M.Cartmell, *Introduction to Linear, Parametric and Nonlinear Vibrations*. Chapman and Hall, 1990.

[20] N. McLachlan, *Theory and Applications of the Mathieu Functions*. Oxford University Press, London, 1951.

[21] K. Turner et al., "Five parametric resonances in a MicroElectro-Mechanical system," *Nature*, vol. 396, no. 6707, pp. 149–156, 12 Nov. 1998.

[22] M. Yu et al., "Realization of parametric resonances in a nanowire mechanical system with nanomanipulation inside a scanning electron microscope," *Physical Review B-Condensed Matter*, vol. 66, no. 7, pp. 073406/1–4, 15 Aug. 2002.

[23] W. Zhang et al., "Effect of cubic nonlinearity on auto-parametrically amplified resonant MEMS mass sensor," *Sensors & Actuators A-Physical*, vol. A102, no. 1-2, pp. 139–150, 1 Dec. 2002.

[24] W.Zhang, R.Baskaran, and K.Turner, "Tuning the dynamic behavior of parametric resonance in a micromechanical oscillator," *Applied Physics Letters*, vol. 82, no. 1, pp. 130–2, 1 Jan. 2003.